A New Design of Composite Pavement with Asphalt Interlayer between CRCP and Cement Treated Base Course

Takayuki Kazato[1], Shiro Motomatsu[2], Naoki Suzaki[2], Tatsuo Nishizawa[3], and Hitomi Taketsu[4]

Abstract

In Japan, composite pavements are adopted in expressways to ensure a long service life with minimum maintenance work. A typical design of the composite pavement utilizes a porous asphalt surface and a CRCP over a cement treated base course (CTB). An investigation on a 20 years old composite pavement revealed that the CTB was damaged due to water penetration and erosion. This finding promoted us to develop a new type of composite pavement, which introduces an asphalt interlayer (AIL) over the CTB to prevent the erosion. A structural design method for the new design of the new composite pavement was developed based on thermal and load stress calculations and fatigue analysis. Full scale test composite pavements were constructed and thermal and load strains measured on the pavements. A 3DFEM model was developed for stress calculation and validated by comparing the calculated and measured strains. The new design method provides 10 % reduction of fatigue damage by introducing AIL. It was also found that the fatigue damage increases six times if AIL is not used and CTB is eroded.

Introduction

In Japan, composite pavements are adopted in expressways to ensure a long service life with minimum maintenance works. A typical design of the composite pavement utilizes a porous asphalt surface and a continuously reinforced concrete pavement (CRCP) over a cement treated base (CTB). A field investigation was conducted on a 20 years old composite pavement to examine the long-term performance of this type of pavement. Figure 1 shows that transverse cracks in CRCP reflecting to the asphalt surface with a spacing of about 600 mm. Figure 2 shows a core taken from the pavement and a gap found between the CRCP and CTB, which demonstrates that the CTB was severely damaged and become granulated due to water penetration and erosion. This finding promoted us to develop a new design of composite pavement, which introduces an asphalt interlayer (AIL) over the CTB to prevent the base erosion.

[1] Nippon Expressway Research Institute Company Limited, 1-4-1 Tadao, Machida, Tokyo, 194-8508, Japan. t.kazato.aa@ri-nexco.co.jp.
[2] West Nippon Expressway Company Limited, 1-6-20 Dojima, Kitaku, Osaka, 530-0003, Japan.
[3] Ishikawa National College of Technology, Tsubata, Ishikawa, 929-0392, Japan. nishi@ishikawa-nct.ac.jp
[4] Sumitomo Osaka Cement Company Limited, 7-1-55 Minamiokajima, Taisyoku, Osaka, 551-0021, Japan

Figure 1. Transverse Cracking on the Asphalt Surface.

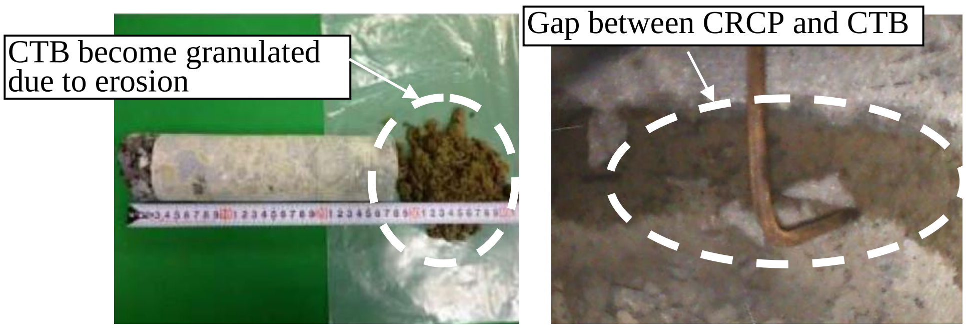

Figure 2. A Core Taken from CRCP and Gap between CRCP and CTB.

A structural design method for the composite pavement was developed based on thermal and load stress calculations and fatigue analysis. A full scale test composite pavement was constructed and thermal and load strains were measured on the pavements. A 3DFEM model was created for the stress calculations and validated by comparing the calculated and measured strains. The research significance of this study is to propose a new design of composite pavement and confirm the benefit of the AIL on the long term performance of the pavement.

Full Scale Test Pavement

Overview of Test Pavement. To compare mechanical behavior of composite pavement with and without AIL, a test composite pavement was constructed. The test pavement has two sections, Section A and Section B, with different base course structures as shown in Figure 1. The base course of Section A was a 40 mm AIL and 160 mm CTB. That of Section B was only a 200 mm CTB. The length of each section was 280 m long. The CTB had an axial compressive strength of 3 MPa. The AIL used a stone mastic asphalt concrete, of which properties are presented in Table 1. A concrete slab with a thickness of 250 mm was placed over both sections. Longitudinal steel bars with a diameter of 16mm were embedded at a third depth from the top of the slab with a spacing of 125mm (0.64% steel reinforcement of cross section area). Transverse steel bars with a diameter of 13 mm were installed at a 300 mm spacing skewed with a 60 degree with respect to the longitudinal direction. The concrete mixture proportion is presented in Table 2. The flexural strength of the concrete was 5.17 MPa.

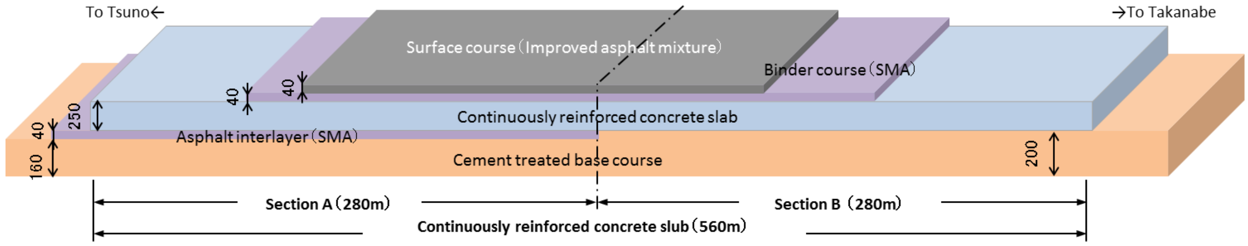

Figure 3. Full Scale Test Composite Pavement

Table 1. Properties of Stone Mastic Asphalt Mixture (SMA).

Item	Value
Optimum asphalt content [%]	6.5
Density [g/cm3]	2.388
Air void [%]	2.5
Marshal stability [kN]	9.70
Flow [1/100cm]	38
Residual stability [%]	90.8

Table 2. Mixture Proportion of Concrete.

Gmax [mm]	Slump [cm]	W/C [%]	s/a [%]	Air [%]	Unit content						Ad [%]
					W	C	S1	S2	G1	G2	
40	4.5	46.1	40	6.0	140	304	293	435	610	499	1.1

Note: Gmax: maximum aggregate size, W: water, C: Cement, S1& S2: Fine aggregate, G1& G2: Coarse aggregate, Ad: Admixture

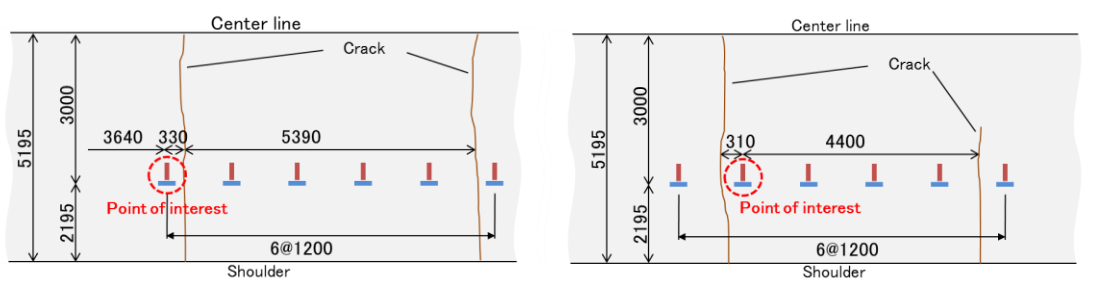

(a) Section A (b) Section B

Figure 4. Measurement Points and Cracks a Month after Concrete Placement.

Figure 5. Sensor Installation at a Measurement Point.

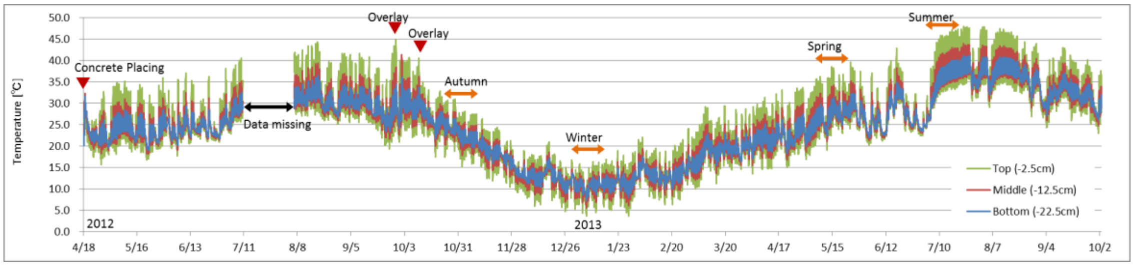

(a) Section A

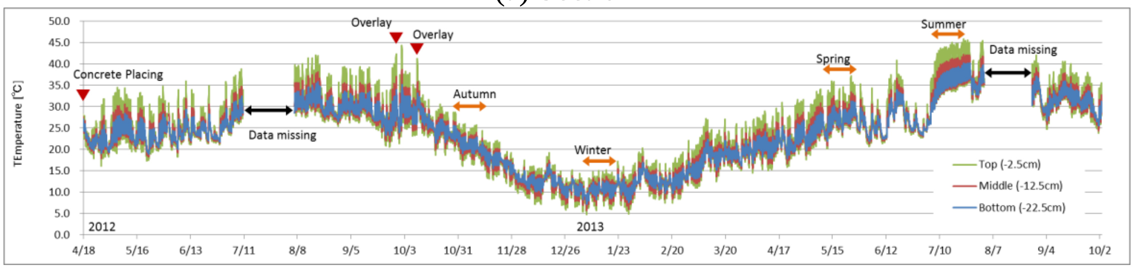

(b) Section B

Figure 6. Measured Temperature Variation for One Year Period.

Measurement Instrumentation. Temperatures and strains in the slab had been continuously measured every one hour since the slab was placed. The time of the placement was 18th April in Section A and 16th April in Section B. At the middle of each section, six measurement points were arranged as shown in Figures 4. Each measurement point had six strain gauges with temperature sensors at 25mm from the top, middle and 25mm from the bottom, as shown in Figure 5, to measure distributions through slab depth of strains in the longitudinal and transverse directions and temperatures.

Few transverse cracks were observed near the measurement points a month after the placement of concrete as shown in Figures 4. The average width of the transverse crack was 0.15mm in Section A, and 0.35mm in Section B.

Temperatures in CRCP. Figure 6 shows temperature changes measured for one year and half after casting concrete. Just after casting, temperatures rapidly increased due to hydration of concrete and in a couple of days temperatures began to fluctuate according to daily air temperature change when the concrete hardened enough. Temperatures in Section B were slightly lower than those in Section A. Amplitude of daily change substantially decreased in October, when the CRCP was overlaid with an 80mm thick asphalt concrete surface.

Strains in CRCP. Measured strains included strains due to hydration and moisture and temperature changes. Daily thermal strain change was extracted by setting a temperature in the morning as an initial one and calculating relative temperature change from the initial one. This operation was done on every day for a period of particular two consecutive days of each season, as presented in Table 3, during which no rainfall was observed. Restraint strain, which causes thermal stress, was estimated from the equation:

$$\varepsilon_r = \varepsilon_m - \alpha \cdot \Delta T \qquad (1)$$

where, ε_r : restraint strain, ε_m : measured strain, α : thermal expansion coefficient of concrete, and ΔT : temperature change from the initial temperature.

Table 3. Representative Period of Analysis for Each Season.

Season	Representative period	
	Start	End
Spring	02/05/2012 8:00	04/05/2012 7:00
Summer	07/08/2012 9:00	09/08/2012 8:00
Autumn	01/11/2012 12:00	03/11/2012 11:00
Winter	31/12/2012 19:00	02/01/2013 18:00

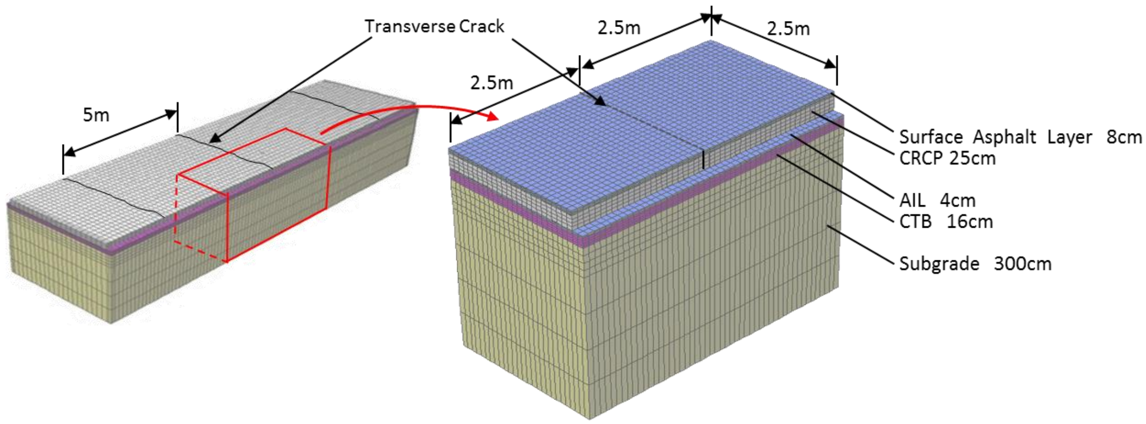

Figure 7. Structural Model for Thermal Stress Analysis.

Elastic Modulus of AIL for Thermal Analysis

In our previous study (Taketsu, et al 2014), the elastic modulus of AIL was identified for the CRCP before overlaying with asphalt surface by comparing measured and calculated strains with 3DFEM model. In this study, the elastic modulus of AIL was identified all over again for CRCP after overlaying with the asphalt surface in the similar way, because the asphalt surface was supposed to affect thermal conditions of the resulted composite pavement.

Analysis Model. A 3DFEM model was created for the simulation as shown in Figure 7, where a half part of the pavement section between the transverse cracks was extracted and meshed. The spacing of transverse crack was assumed 5 m as observed in Figure 3. Four side of the meshed region were symmetric plane, where displacement perpendicular to the plane was fixed and other displacements parallel to the plane were free. All displacements on the bottom of the region were fixed. All displacements on the right side of the concrete slab were free.

Input data for the simulation including material parameters is presented in Table 4. The elastic modulus of AIL was varied in 100, 1000 and 5000 MPa. The elastic modulus of asphalt surface layer was determined to be 100 MPa from the whole year comparison between the measured and calculated strains at the bottom of the concrete slab. Standard values of elastic modulus of CTB and subgrade were used.

Table 4. Input Data for the Simulation.

Structural Layer	Parameter [Unit]	Value
Asphalt surface layer	Elastic Modulus [MPa]	100
	Poisson Ratio	0.35
	Thermal Expansion Coeff. [/^{o}C]	0.00003
	Density [kN/m^3]	23
Concrete slab	Elastic Modulus [MPa]	300000
	Poisson Ratio	0.2
	Thermal Expansion Coeff. [/^{o}C]	0.00001
	Density [kN/m^3]	24
AIL	Elastic Modulus [MPa]	100, 1000, 5000
	Poisson Ratio	0.35
	Thermal Expansion Coeff. [/^{o}C]	0.00003
	Density [kN/m^3]	23
CTB	Elastic Modulus [MPa]	3,000
	Poisson Ratio	0.2
Subgrade	Elastic Modulus [MPa]	80
	Poisson Ratio	0.35

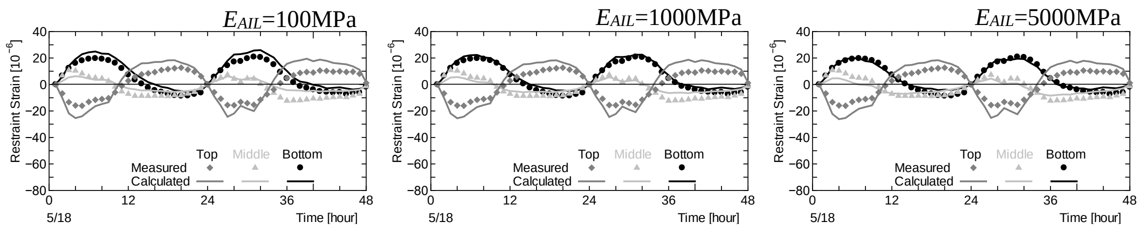

(a) Spring

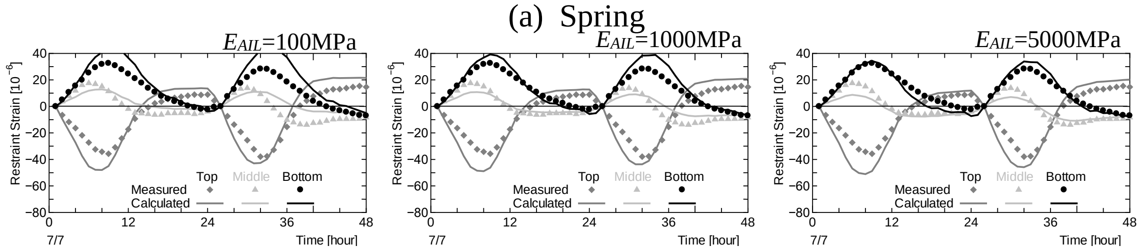

(b) Summer

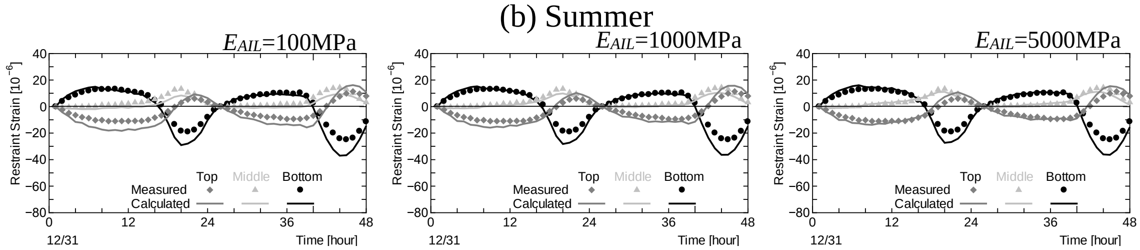

(c) Winter

Figure 8. Comparisons of Measured and Calculated Restraint Strains.

Identification of Elastic Modulus of AIL Figure 8 compares the measured and calculated restraint strains. Looking at the bottom strains, the calculated strains with an elastic modulus of 5000 MPa is the closest to the measured strains. From the comparison, the value of elastic modulus of AIL was determined to be 5000 MPa.

Fatigue Damage of CRCP

The effect of AIL on fatigue resistance of the composite pavement was examined from the fatigue analysis of CRCP. Relative frequencies of the load and thermal stresses of the concrete slab under the asphalt surface were calculated and fatigue damage was estimated as (Ozeki, et al 2010 and Nishizawa 2012):

$$F_d = \sum_p \sum_l \sum_{\sigma T} \frac{f_p f_l f_{\sigma T} N_{total}}{N_{allowable}(\sigma_{pl}, \sigma_T, \sigma_a)} \tag{2}$$

where,

Fd = fatigue damage,

f_p = relative frequency of a wheel load *p*,

f_l = relative frequency of a wheel position *l*,

f_{σ_T} = relative frequency of thermal stress, σ_T .

σ_{pl} = load stress that is generated by a wheel load of *p* located at a position *l*,

σ_a = flexural strength of concrete, and

N_{total} = total number of wheel loads expected for a design period.

$N_{allowable}$ is allowable number of load repetition estimated from fatigue curve of concrete and expressed as follows:

$$\log_{10} N_{allowable} = \frac{a - SL}{b} \tag{3}$$

where,

$SL = \dfrac{\sigma_{pl} + \sigma_T}{\sigma_a}$,

$a = 1.1136 + 0.00165 P_f$, $b = 0.09722 - 0.0002 P_f$ and,

P_f =failure probability (=10%).

Load Stress Calculation. In this examination, the structural model was reconstructed with a transverse crack spacing of 0.6 m based on the field observation result shown in Figure 1. Figure 9 shows the structural model used in both the load and thermal stress calculations. We considered a case where a part of CTB was deteriorated, which was found in the field investigation as shown in Figure 2. It was assumed that its elastic modulus reduced to one tenth of the initial value (NCHRP 2004). Therefore three cases of base course condition were examined: Case A (Section A), Case B (Section B) and Case C (Section B deteriorated).

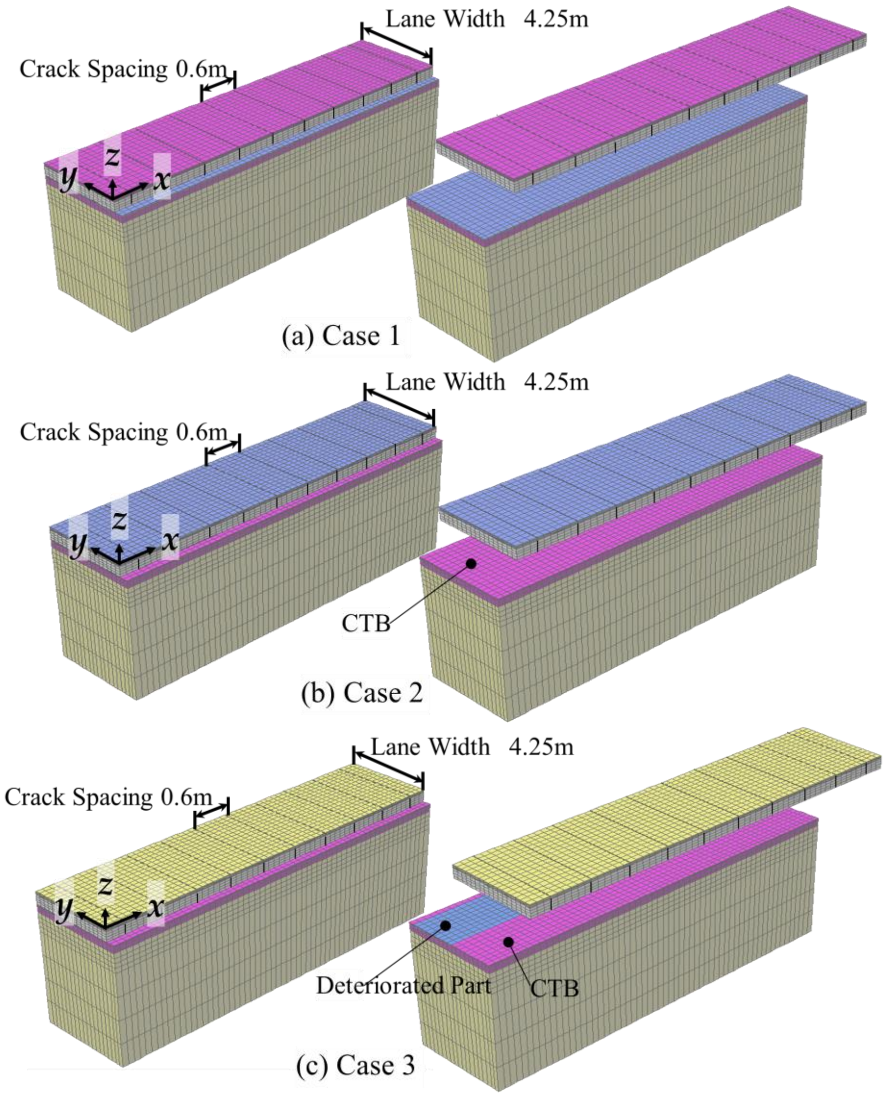

Figure 9. Structural Model for Stress Calculations.

Since the thermal stress was larger than the load stress, the combined stress ($=\sigma_{pl}+\sigma_T$) would become the maximum at the location where the maximum thermal stress occurs. Therefore, we assumed that wheels pass most relative frequently (f_l =0.5) at that location and f_l =0.25 at other locations (positions 300 mm offset right and left from the most frequent location). Figure 10 shows the bending stress distributions at the bottom of the slab for each loading location.

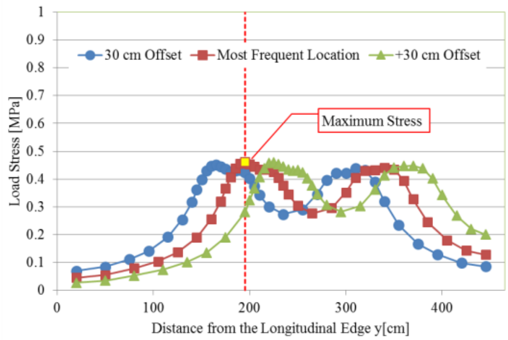

(a) Case 1

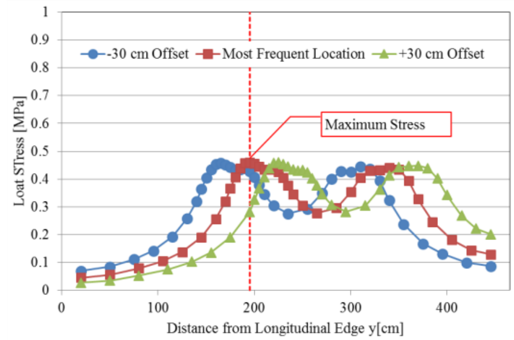

(b) Case 2

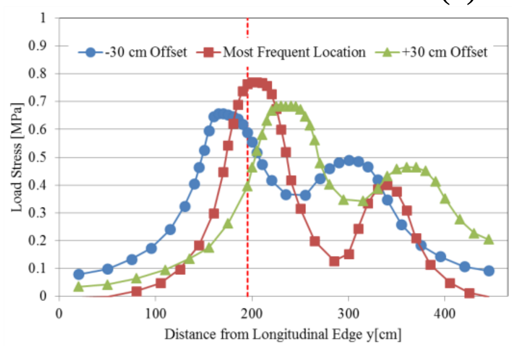

(c) Case 3

Figure 10. Bending Stress Distributions at the Bottom of the Slab for Each Loading Location.

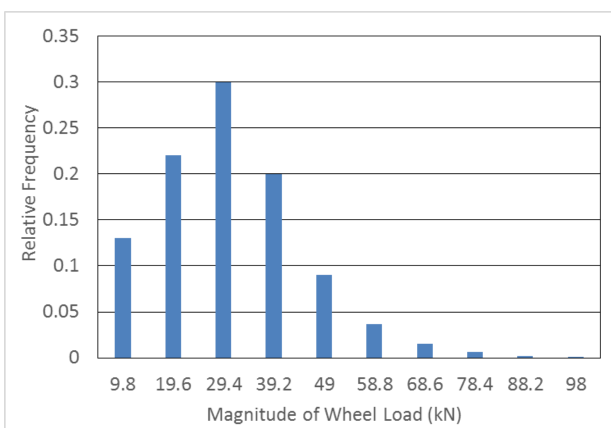

Figure 11. RFD of Axle Load.

The relative frequency distribution (RFD) of axle load, f_p, was assumed as shown in Figure 11, which is the standard distribution specified in Japanese pavement design guide (Japan Road Association 2006).

The elastic moduli of asphalt surface layer and AIL were varied depending on the average temperature in the layer in each season. Their values can be estimated from the following equations (East, Central, and West Nippon Express Highway Companies Limited, 2012):

$$E_1 = -337.887 \cdot \ln t - 51.1976 \cdot T + 1933.907$$
$$E_2 = -783.151 \cdot \ln t - 70.564 \cdot T + 2409.832 \qquad (4)$$

where, E_1 = elastic modulus of porous asphalt surface layer
E_2 = elastic modulus of AIL (stone mastic asphalt concrete),
t =loading period and (=0.02 sec.),
T =average temperature of asphalt mixture for each season.
In the 3FEM calculation, asphalt surface layer and concrete slab were combined into a concrete slab with an equivalent thickness by using the combined plate theory (Nishizawa 2010).

Table 5 summarizes the input data for the stress calculation. Elastic moduli of surface asphalt layer and AIL were determined with Eq. (4) and average temperature of each season. The spring constant of transverse crack was varied between winter and the other seasons. All interfaces between layers were assumed to be bonded. The elastic modulus of the weak part of CTB was 300 MPa that is one tenth of the normal one.

The load stress, σ_{pl} , was calculated for the wheel load magnitude, *p*, and wheel load location, *l*, using the structural model. The corresponding relative frequency, f_{pl}, can be estimated by $f_p \times f_l$.

Table 5. Input Data for Load Stress Calculation.

Structural Layer	Parameter [Unit]	Value
Asphalt surface layer	Elastic Modulus [MPa]	2383 (spring), 1984 (summer), 2736 (autumn), 3064 (winter)
	Poisson Ratio	0.35
	Thermal Expansion Coeff. [/ºC]	0.00003
	Density [kN/m^3]	23
Concrete slab	Elastic Modulus [MPa]	300000
	Poisson Ratio	0.2
	Thermal Expansion Coeff. [/ºC]	0.00001
	Density [kN/m^3]	24
Transverse Crack	Spring Constant [MPa/m]	1000 (in winter) 100000 (other seasons)
AIL	Elastic Modulus [MPa]	3300 (spring),2700 (summer), 3800 (autumn), 4600 (winter)
	Poisson Ratio	0.35
	Thermal Expansion Coeff. [/ºC]	0.00003
	Density [kN/m^3]	23
CTB	Elastic Modulus [MPa]	3000 (normal) 300 (deteriorated)
	Poisson Ratio	0.2
Subgrade	Elastic Modulus [MPa]	80
	Poisson Ratio	0.35

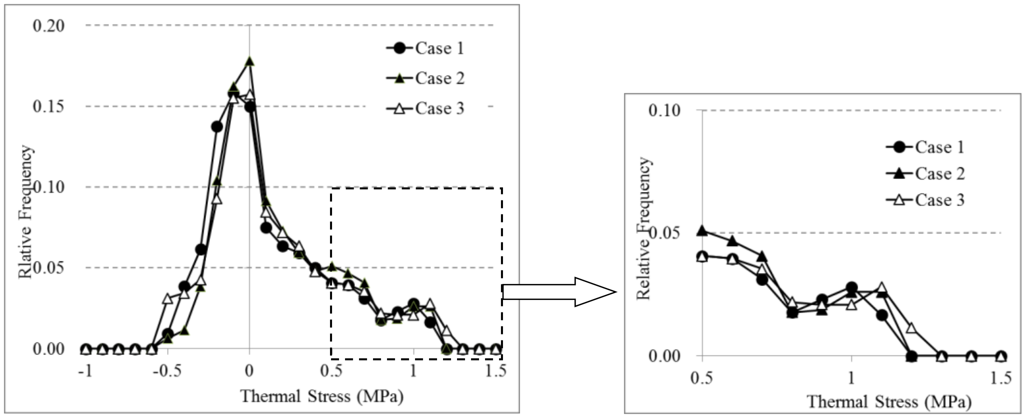

Figure 12. RFDs of Thermal Stress at the Bottom of Slab.

Table 6. Estimated Fatigue Damage.

Case	Base Course Condition	F_d	F_d / Case 2
1	AIL	0.094	0.88
2	CTB sound	0.107	1.00
3	CTB deteriorated	0.646	6.04

Thermal Stress Calculation

RFD of thermal stress at the bottom of CRCP was obtained with the same structural model as that used in the load stress calculation. The measured temperatures in CRCP were input into the model and the thermal stresses were calculated every one hour during the representative 10 days of each season From the calculated stresses, the RFDs obtained is shown in Figure 12.

Fatigue Damage. Fatigue damage F_d for a design period of 40 years was estimated using the RFDs of wheel and thermal stresses obtained in the previous sections according to Eq. (2). The results are summarized in Table 6, where F_d and ratio of F_d for each case to that of Case 2 are presented. F_d for all cases are less than 1.0, meaning that crack would not appear for 40 years. Case 3 exhibits relatively high F_d, six times high as that of Case 2. This means that the deterioration of CTB significantly accelerates the fatigue damage of CRCP. F_d of Case 1 is about 10 % less than that of Case2, which is smaller difference than expected. That means that structural benefit of AIL is not so great comparing to CTB, as far as the base structure remains sound during the service period.

Summary and Conclusion

In this study, structural design of a new composite pavement that uses AIL between CRCP and CTB was performed. Fatigue damage, F_d , was estimated for three cases; Case 1 with AIL and CTB, Case 2 with sound CTB and Case 3 with deteriorated CTB. F_d of Cases 1 and 2 were very low, much less than 1.0 for a design period of 40 years, which confirms a high structural durability of this type of pavement. However, F_d of Case 3 was relatively high, which means that the deterioration of CTB significantly accelerates the fatigue damage of CRCP. The primary conclusion of this study might be that a durable base course is crucial to ensure good long term performance of the composite pavement with asphalt surface and CRCP.

References

East, Central, and West Nippon Express Highway Companies Limited, (2012) *Design specifications of pavement*, Volume 1, Research Institute of Express Highway Limited, Japan.

Japan Road Association, (2010) *Pavement Design Guide.* Maruzen Publishing Co.

NCHRP (2004) "*Guide for Mechanistic-Empirical Design of New and Rehabilitated Pavement Structures.*" Part 2, Chapert 2.,NCHRP, TRB. <http://onlinepubs.trb.org/onlinepubs/archive/mepdg/guide.htm> (Sept. 20, 2015)

Ozeki, T., Nishizawa, T., and Matsui, K. (2010) "Effects of Nonlinearity of Temperature Distribution in Thick Concrete Slab on Fatigue Damage." *Proc 7th International DUT-Workshop on Design and Performance of Sustainable and Durable Concrete Pavements*, Hotel Alcazar de la Reina, Carmona.

Nishizawa, T., Koyanagawa, M., Takeuchi, Y., and Kimura, M. (2005). "Study on Mechanical Behavior of Dowel Bar in Transverse Joint of Concrete Pavement." *Proc., 7th International Conference on Concrete Pavement*, Orland Florida, pp. 571-588.

Nishizawa, T., Ozeki, T., Katoh, K., and Matsui, K. (2009) "Finite Element Model Analysis of Thermal Stresses of Thick Airport Concrete Pavement Slabs." *J. the Transportation Research Board*, No.2095, Transportation Research Board.

Nishizawa, T., Shimeno, S., Komatsubara, A., and Koyanagawa, M. (2010) "Study on design method of composite pavement with CRC base." *Journal of Pavement Engineering*, Japan Society of Civil Engineers, Vol.2.

Nishizawa, T., Ozeki, T., Matsui, K., and Kawano H. (2012) "Effects of Non-Linear Thermal Stress on Fatigue Damage of Airport Concrete Pavements" *Proc., 10th International Conference on Concrete Pavements,* Quebec City, Canada.

Taketsu, H., Kazato, T., Motomatsu, S., Nishizawa, T., and Fumoto, T. (2014) "Mechanical Effect of Thin Asphalt Interlayer on Thermal Stresses of Continuously Reinforced Concrete Slab" *Proc. 93th Annual Meeting of Transportation Research Board*, Washington D.C.